Clinical and Translational Radiation Oncology 49 (2024) 100861

Contents lists available at ScienceDirect

Clinical and Translational Radiation Oncology

journal homepage: www.sciencedirect.com/journal/clinical-and-translational-radiation-oncology

Anatomical and dosimetric variations during volumetric modulated arc therapy in patients with locally advanced nasopharyngeal carcinoma after induction therapy: Implications for adaptive radiation therapy

Shuhan Zhao [a,1], Jun Han [a,1], Zhiyong Yang [a,b,c], Xi Chen [d,e], Xixi Liu [a], Fangyuan Zhou [a], Yajie Sun [a], Ye Wang [a], Gang Liu [a,b,c], Bian Wu [a,b,c], Sheng Zhang [a,c], Jing Huang [a,c,*], Kunyu Yang [a,b,c,*]

[a] Cancer Center, Union Hospital, Tongji Medical College, Huazhong University of Science and Technology, Wuhan 430022, China
[b] Hubei Key Laboratory of Precision Radiation Oncology, Union Hospital, Tongji Medical College, Huazhong University of Science and Technology, Wuhan 430022, China
[c] Institute of Radiation Oncology, Union Hospital, Tongji Medical College, Huazhong University of Science and Technology, Wuhan 430022, China
[d] School of Health, Brooks College (Sunnyvale), United States
[e] Department of Epidemiology and Statistics, School of Public Health, Medical College, Zhejiang University. China

ARTICLE INFO

Keywords:
Nasopharyngeal carcinoma
Adaptive radiation therapy
Volumetric modulated arc therapy
Anatomical and dosimetric changes
Replanning

ABSTRACT

Purpose: To investigate anatomical and dosimetric changes during volumetric modulated arc therapy (VMAT) in patients with locally advanced nasopharyngeal carcinoma (LA-NPC) after induction therapy (IT) and explore characteristics of patients with notable variations.

Materials and methods: From July 2021 to June 2023, 60 LA-NPC patients undergoing VMAT after IT were retrospectively recruited. Adaptive computed tomography (aCT), reconstructed from weekly cone-beam computed tomography(CBCT), facilitates recontouring and planning transplantation. Volume, dice similarity coefficients, and dose to target volumes and organs at risk(OARs) on planning CT(pCT) and aCT were compared to identify changing patterns. Multivariate logistic regression was used to investigate risk factors.

Results: The volumes of PGTVnasopharynx (PGTVp), PGTVnode (PGTVn), ipsilateral and contralateral parotid glands decreased during VMAT, with reductions of 2.25 %, 6.98 %, 20.09 % and 18.00 %, respectively, at 30 fractions from baseline ($P < 0.001$). After 25 fractions, D99 and D95 of PGTVn decreased by 7.94 % and 4.18 % from baseline, respectively, while the Dmean of ipsilateral and contralateral parotid glands increased by 7.80 % and 6.50 %, marking the peak rates of dosimetric variations ($P < 0.001$). The dosimetric fluctuations in PGTVp, the brainstem, and the spinal cord remained within acceptable limits. Furthermore, an initial BMI $\geq$ 23.5 kg/m^2 and not-achieving objective response (OR) after IT were regarded as risk factors for a remarkable PGTVn dose reduction in the later stages of VMAT.

Conclusions: Replanning for post-IT LA-NPC patients appears reasonable at 25F during VMAT. Patients with an initial BMI $\geq$ 23.5 kg/m^2 and not-achieving OR after IT should be considered for adaptive radiation therapy to stabilize the delivered dose.

Introduction

Radiotherapy remains the mainstay of treatment for non-metastatic nasopharyngeal carcinoma (NPC) due to its high radiotherapy sensitivity and the challenging operability of its unique anatomical location [1–3]. Emerging as the mainstream radiotherapy technique for NPC, intensity-modulated radiotherapy (IMRT) offers superior dose conformity and steeper dose variations, enabling patients to achieve higher local tumor control and prolonged survival while reducing radiation-induced injury to organs at risk (OARs) [1–4]. Furthermore,

* Corresponding authors at: Cancer Center, Union Hospital, Tongji Medical College, Huazhong University of Science and Technology, 1277 Jiefang Avenue, Wuhan 430022, Hubei, China.
E-mail addresses: hjtopaz@hotmail.com (J. Huang), yangkunyu@hust.edu.cn (K. Yang).
[1] These authors contributed equally to this work.

https://doi.org/10.1016/j.ctro.2024.100861
Received 29 May 2024; Received in revised form 13 September 2024; Accepted 16 September 2024
Available online 17 September 2024

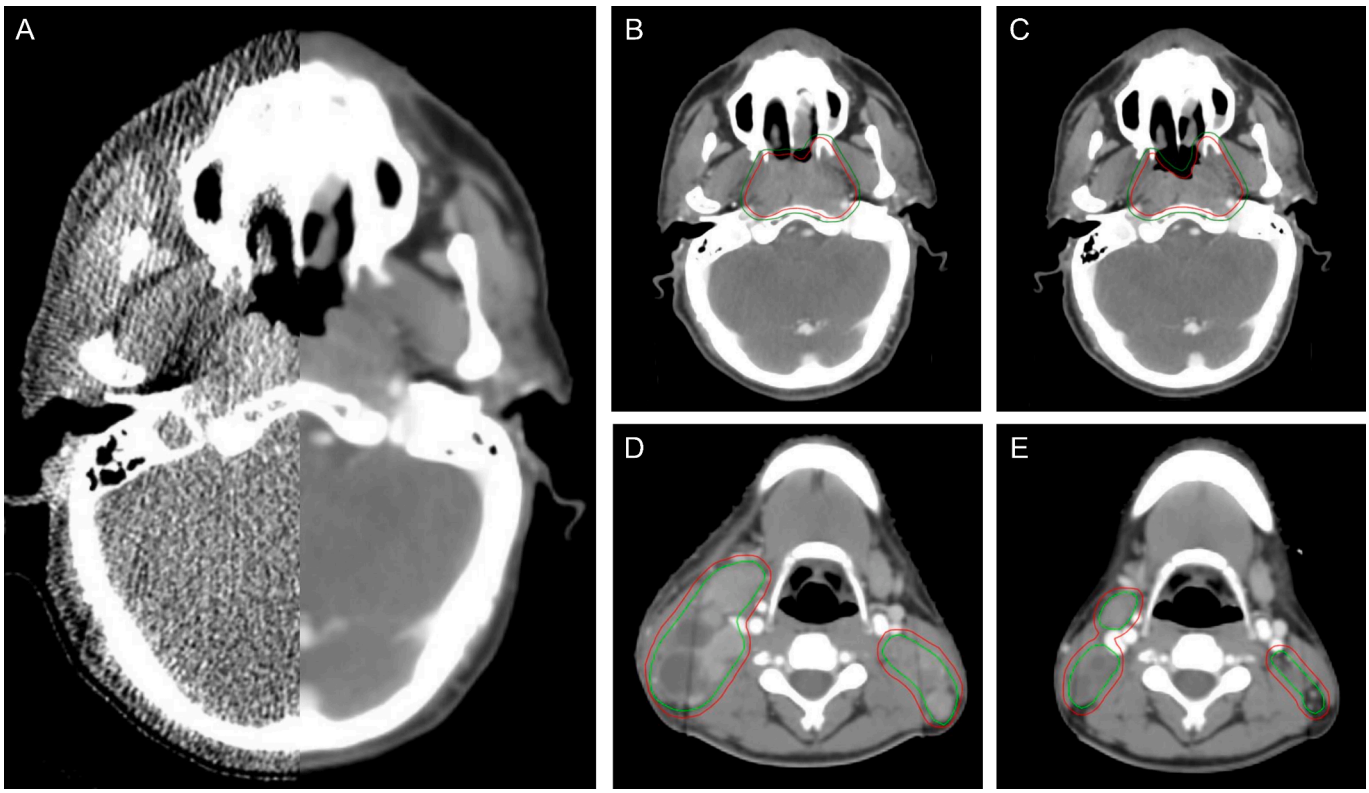

Fig. 1. CBCT reconstruction and TVs modification. (A) Rigid registrations between CBCT (left) and aCT (right); (B–C) An example of TVs recontouring (Red line: GTVp, Green line: PGTVp), B: Before radiotherapy, C: After radiotherapy; (D–E) An example of TVs recontouring (Red line: PGTVn, Green line: GTVn), D: Before radiotherapy, E: After radiotherapy. (For interpretation of the references to colour in this figure legend, the reader is referred to the web version of this article.)

volumetric modulated arc therapy (VMAT), an advanced iteration of IMRT, significantly shortens treatment times. In addition to improving the efficiency and accuracy of radiotherapy, VMAT imposes higher standards for quality control and assurance [1,5]. Therefore, ensuring the accuracy of target volumes (TVs) and stability of the delivered doses is imperative for the effectiveness and safety of VMAT.

Studies have demonstrated that over a 7-week radiotherapy course, patients with NPC experience tumor regression and changes in body weight and shape [6–10]. These alterations potentially result in the migration of TVs out of the high-dose region and OARs into the high-dose region, leading to decreased doses to the TVs and increased doses to the OARs [9,11–13]. To address the challenges arising from variations in radiotherapy fractions, Yan et al. introduced adaptive radiation therapy (ART) in 1997 [14]. ART aims to achieve precise radiation therapy by employing image-guided radiation therapy and evaluating patient feedback, such as variations in tumor dimensions, morphology, and location, to optimize the radiotherapy plan [5,14,15]. ART is categorized as online and offline ART [14,15]. Online ART requires real-time and efficient plan adjustment within a few minutes. However, due to limitations in technology and equipment, offline ART is used more widely, in which appropriate modifications are made to the plan or TVs at specific time points [15]. Despite being a labor-intensive and highly complex procedure, the benefits of ART do not necessarily increase with the frequency of adaptation [1,15–18]. Consequently, repositioning and replanning at a fixed time point to avoid significant dose variations in TVs and OARs seems to be a more economical and favorable ART technique for head and neck cancers [1,15–18]. However, there is a lack of consistent conclusions regarding dosimetric changes in the TVs and OARs during radiation therapy in patients with NPC, leading to controversies about the necessity and modality of ART implementation.

Approximately 55.6–94.5 % of patients with locally advanced nasopharyngeal carcinoma (LA-NPC) can achieve objective response (OR) during induction therapy (IT), implying substantial decreases in tumor volumes before the commencement of radiotherapy [19–22]. Moreover, a recent study proposed that IT plays a pivotal role in mitigating volume reductions in the gross tumor volume (GTV) and clinical target volume (CTV), minimizing dosimetric drift during concurrent chemoradiotherapy (CCRT) [23]. Therefore, the pattern of variations in TVs and OARs during radiotherapy in patients after IT may be different from that in patients who receive CCRT directly. However, relevant studies for post-IT LA-NPC patients remain lacking. The present study addressed this problem by retrospectively investigating anatomical and dosimetric changes in the TVs and OARs during VMAT in post-IT LA-NPC patients and characterizing patients with significant variations to provide inspiration for ART.

Methods and materials

Patient characteristics

This retrospective analysis focused on patients initially diagnosed at our center between July 2021 and June 2023 who met the following criteria: 1. Pathologically diagnosed with NPC featuring non-keratinizing undifferentiated carcinoma (NKUC). 2. Classified as stage III–IVa according to the 8th edition of the American Joint Committee on Cancer (AJCC) guidelines. 3. TVs contoured by the same two radiotherapists. 4. Received VMAT using a Varian Halcyon linear accelerator after IT with weekly cone-beam computed tomography (CBCT) scanning. Patients with tumors at other sites, severe underlying diseases, radiotherapy interruption exceeding two weeks, replanning during radiotherapy, or missing data were excluded. Approval for this research was obtained from the Ethics Committee of Union Hospital, Tongji Medical College, Huazhong University of Science and Technology.

Localization and CT simulation

The included patients underwent localization and an initial CT simulation (CT-sim) scan (iCT) before IT. Another CT-sim scan was conducted after IT to create a planning CT (pCT) for contouring. Patients were placed in the supine position with their heads and necks resting on A/C positioning pillows and immobilized using T-shaped thermoplastic masks encompassing the head, neck, and shoulders. Subsequently, an enhanced scan was performed on a large-aperture 16-slice helical CT machine (Philips Medical Systems, Netherlands) to simulate positioning. The scan covered the range from the top of the skull to the aortic arch, featuring a layer thickness and spacing of 3 mm, which was transferred to the Eclipse treatment planning system (TPS, version 8.6; Varian Medical System, Palo Alto, Calif) for contouring and VMAT plan design.

Definition of TVs and planning delivery

Meticulous contouring of the TVs and OARs was performed layer-by-layer on pCT by the same senior radiation oncologist concerning the magnetic resonance imaging(MRI)/ computed tomography(CT) fusion images and revised by another physician. The GTV comprised primary tumors (GTVp) and lymph nodes (GTVn) identified through radiographic, endoscopic, and clinical examinations. The CTV was further delineated into high-risk (CTV1) and low-risk (CTV2) areas. The planning target volume (PTV) incorporated the GTV and CTV, featuring a 3-mm expansion of the corresponding TVs to form the PGTV, PCTV1, and PCTV2. For the spinal cord and brainstem, outward expansions of 5 mm and 1 mm were applied to create the SC and BC, respectively, representing the planning organ at risk volume (PRV). All structures were contoured according to the 2021 Chinese Society of Clinical Oncology (CSCO) guidelines and the international guidelines for TVs delineation in NPC [24–26].

The prescribed doses for the PGTVp, PGTVn, PCTV1, and PCTV2 were 70 Gary (Gy) in 33 fractions (F, 2.12 Gy per fraction), 70 Gy in 33F (2.12 Gy per fraction), 60 Gy in 33F (1.82 Gy per fraction), and 54 Gy in 33F (1.64 Gy per fraction), respectively. Following specific dose constraints for OARs, the volume of the spinal cord receiving 45 Gy or more, and the volume of the brainstem, optic nerves, and optic chiasm receiving 54 Gy or more, should be less than 1 %. The mean dose to the parotid gland should be maintained below 28 Gy. The VMAT plan was created using Eclipse TPS to ensure that 95 % of the PTV is adequately covered by 100 % of the prescribed dose.

CBCT scan and reconstruction

VMAT plans were delivered on the Varian Halcyon linear accelerator, and CBCT images were acquired in the treatment position before each radiotherapy fraction. CBCT scans were performed weekly (at 1F, 5F, 10F, 15F, 20F, 25F, and 30F) and imported into the Velocity software (version 4.0, Varian Medical System, Palo Alto, Calif) for reconstruction to create adaptive CTs (aCT1, aCT2, aCT3, aCT4, aCT5, aCT6, and aCT7), as illustrated in Fig. 1A. Rigid registrations were established between aCTs and pCT, which was subsequently imported into the Eclipse TPS for recontouring and dose calculation.

Recontouring and planning migration

The original TVs from the pCT were replicated onto the aCTs, and the contours of the TVs and OARs were modified based on the anatomical changes observed on the aCTs. The primary goal in recontouring the TV was to address the anatomical position and cavity changes resulting from the tumor regression, while also preserving the integrity of the tumor bed as much as possible (Fig. 1B–E). This approach was also applied to contouring TVs in iCT scans before the commencement of IT.

The PGTVn of positive lymph nodes (PGTVnp), high-risk lymph nodes (PGTVnh), and suspicious lymph nodes (PGTVns) were individually delineated within the PGTVn. Positive lymph nodes included high-risk lymph nodes, lymph nodes in clusters, and those with a minimal diameter ≥10 mm on cross-sectional images (the last criterion for lymph nodes was extended to 11 mm in the subdigastric region)[27]. High-risk lymph nodes were defined as central necrosis or circumferential enhancement, and extranodal extension (ENE) marked by irregular enhancement of margins, partial or total loss of surrounding fat interstitium, or fusion of the lymph nodes [28,29]. Suspicious lymph nodes did not meet the criteria for positive or high-risk nodes but were included in the GTV. Parotid glands were categorized as ipsilateral (Parotid_I) or contralateral (Parotid_C), depending on the presence or absence of positive lymph nodes among the Level II cervical lymph nodes. If the patient has bilateral Level II positive lymph nodes, both parotid glands are considered ipsilateral; conversely, if there are no positive lymph nodes in Level II on either side, both parotid glands are considered contralateral. The SC was further divided based on spinal cord segments: SC12 (cervical1–2), SC35 (cervical 3–5), SC6 (cervical 6), SC7 (cervical 7), and SCT (thoracic spinal cord).

The original plans were transferred to the aCTs to create hybrid plans, on which the dose-volume histograms were recalculated based on

Table 1
Patient characteristics.

Characteristics	No. of patients (n = 60)	Percent
Sex		
Male	48	80.00 %
Female	12	20.00 %
Age (years)		
Range	28–72	
Median	52	
Histopathological type		
NKUC	60	100.00 %
T stage		
T1	2	3.33 %
T2	9	15.00 %
T3	34	56.67 %
T4	15	25.00 %
N stage		
N0	2	3.33 %
N1	34	56.67 %
N2	18	30.00 %
N3	6	10.00 %
Clinical stage		
III	40	66.67 %
IVA	20	33.33 %
Induction therapy		
GP	17	28.33 %
GP+PD-1 inhibitor	9	15.00 %
GP+PD-1 inhibitor + Endostatin	1	1.67 %
T	1	1.67 %
TP	20	33.33 %
TP+PD-1 inhibitor	12	20.00 %
Concurrent therapy		
DDP	28	46.67 %
DDP+nimotuzumab	7	11.67 %
DDP+Endostatin	1	1.67 %
DDP+PD-1 inhibitor	9	15.00 %
DDP+PD-1 inhibitor + nimotuzumab	2	3.33 %
nimotuzumab	2	3.33 %
NDP	4	6.67 %
NDP+nimotuzumab	3	5.00 %
NDP+PD-1 inhibitor	2	3.33 %
PD-1 inhibitor	2	3.33 %
Response after IT		
OR	39	65.00 %
CR	1	1.67 %
PR	38	63.33 %
SD	21	35.00 %

NKUC: non-keratinizing undifferentiated carcinoma, GP: gemcitabine and cisplatin/nedaplatin; PD-1: programmed cell death protein-1; T: paclitaxel; TP: paclitaxel and cisplatin/nedaplatin; DDP: cisplatin; NDP: nedaplatin; IT: induction therapy, OR: objective response; CR: complete response; PR: partial response; SD: stable disease.

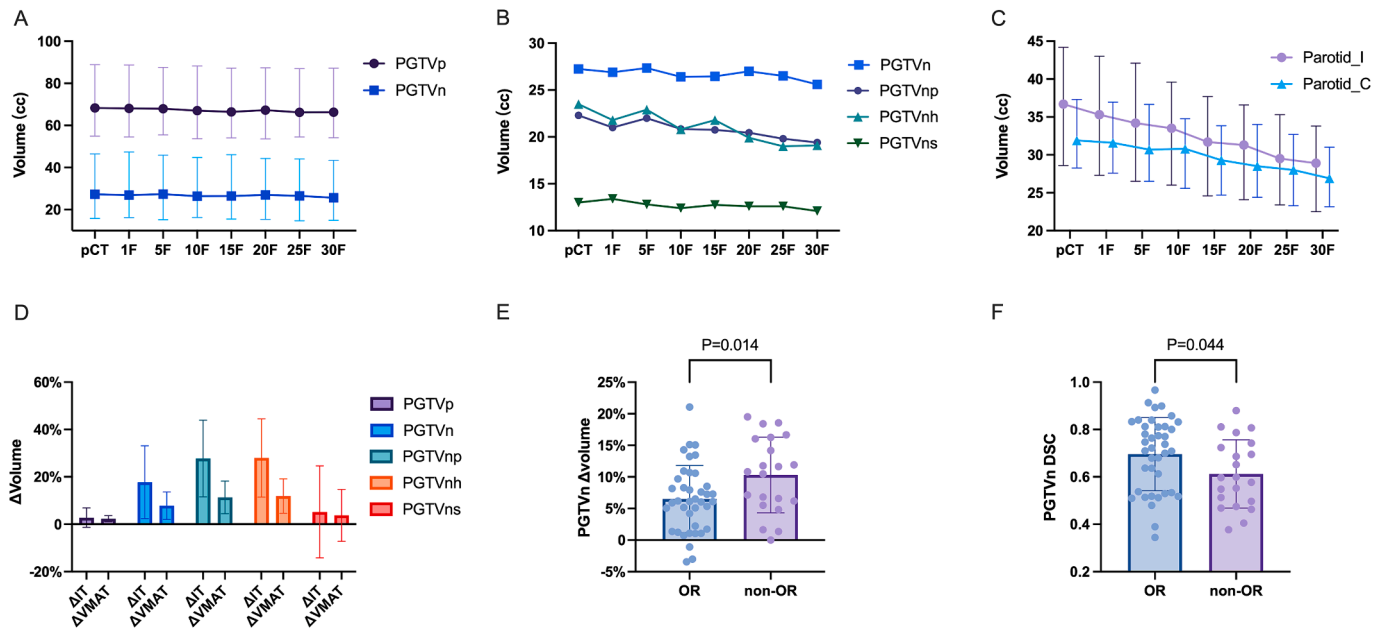

Fig. 2. Volumetric variations (A) Volumetric changes in PGTVp and PGTVn based on median (P25, P75); (B) Volumetric changes in PGTVn, PGTVnp (the PGTVn of positive lymph nodes), PGTVnh (the PGTVn of high-risk lymph nodes), and PGTVns (the PGTVn of suspicious lymph nodes) based on median; (C) Volumetric changes in parotid glands based on median (P25, P75); (D) Comparison of percent volumetric change in TVs during IT and VMAT based on mean ± SD; ΔIT: percentage decrease in volume during IT compared to pre-IT; ΔVMAT: percentage decrease in volume during VMAT compared to pre-VMAT; (E) Comparison of volumetric changes in PGTVn during VMAT in OR and not-achieving OR patients; (F) Comparison of PGTVn DSC at 30F in OR and not-achieving OR patients.

the recontouring curves to determine the actual delivered dose. In addition, relevant parameters, such as volume and deformation information, were collected and analyzed.

Evaluation and statistical analysis

Tumor responses were evaluated according to the response evaluation criteria in solid tumors (RECIST) guideline, version 1.1,where OR was defined as complete response (CR) or partial response (PR). Dose to 99 % (D99) and 95 % (D95) of the volume were applied to assess the delivered doses of TVs. For the parotid gland, mean dose (Dmean) and volume percentage receiving 30 Gy (V30) were collected, while maximum dose (Dmax) and dose received in a volume > 0.1 cc (D0.1 cc) were gathered for the SC and the BC. Deformation and displacement were assessed using dice similarity coefficients (DSCs), which measure the degree of overlap between two contours on a scale from 0 to 1. A DSC of 1 indicates complete overlap, whereas 0 signifies no intersection between the contours [30]. Notably, a DSC<0.7 indicates a substantial morphological difference [31].

Statistical analyses were performed using SPSS version 26.0 (SPSS Inc., Chicago, IL, USA). Data are described as mean ± standard deviation (SD) or median (P25, P75) and analyzed using paired *t*-tests or the Wilcoxon test based on normality test results. Generalized estimating equations were applied to repeated measures data, and Spearman's correlation was employed for correlation analysis. Cutoff values were determined by the receiver operating characteristic (ROC) curves, and risk factors were explored through logistic regression. Statistical significance was set at P<0.05.

Results

Between July 2021 and June 2023, 97 patients with NPC underwent contouring by the same two radiation oncologists and received VMAT using the Varian Halcyon linear accelerator at our center. After excluding 4 patients with non-NKUC, 12 patients with non-locally advanced disease, 8 patients with replanning during radiotherapy, 2 patients with other tumors, 3 patients with interrupted radiotherapy, 5 patients without IT, and 3 patients with incomplete data, 60 patients with NPC were finally included. Table 1 outlines their characteristics, with 80 % of the participants being male with a median age of 52 years. They were categorized as stages III–IVA, with 66.7 % falling into stage III. All patients received IT before VMAT, and 36.7 % (22/60) of them received programmed cell death protein-1 (PD-1) inhibitors during IT.

Volumetric variations

During the final week of VMAT, the volume of the PGTVp and PGTVn regions decreased by 2.25 % (1.37 %, 3.09 %) and 6.98 % (4.27 %, 11.73 %), respectively, compared to baseline (P < 0.001, Fig. 2A and Table S2), with a more pronounced reduction in PGTVn than PGTVp (P < 0.001, Tables S1–S2). At 30F, the volumes of PGTVnp and PGTVnh decreased by 9.94 % (7.10 %, 17.13 %) and 9.71 % (6.06 %, 18.72 %) from baseline, respectively, and the decrease was more significant than that of PGTVn (P<0.001), whereas PGTVns experienced a lesser decrease than PGTVn (P = 0.002, Fig. 2B and Tables S1–S2). Furthermore, during the final week of VMAT, the ipsilateral and contralateral parotids showed volumetric reductions of 20.09 ± 7.31 % and 18.00 ± 7.23 %, respectively (P<0.001, Fig. 2C and Table S1).

The objective response rate (ORR) following IT was 65.00 % (39/60), compared to 72.72 % (16/22) for patients receiving immunotherapy (Table 1). The volumetric decreases of PGTVn, PGTVnp, and PGTVnh during VMAT were less pronounced than during IT (6.98 % vs. 17.73 %, 9.94 % vs. 27.75 %, and 9.71 % vs. 28.00 %, respectively; P<0.001, Fig. 2D and Table S3). Additionally, compared to patients who achieved OR after IT, not-achieving OR patients presented more volume reductions (6.51 % vs. 10.30 %; P=0.014) and smaller DSCs (0.70 vs. 0.61; P=0.044) of PGTVn during VMAT (Fig. 2E–F).

Dosimetric variations

No obvious alternation was observed in D99 of the PGTVp during radiotherapy (P=0.66), whereas D95 showed only minor fluctuations from baseline during the first and last weeks of VMAT (P<0.001 and P = 0.041, Fig. 3A and Table S4). In contrast, PGTVn showed significant

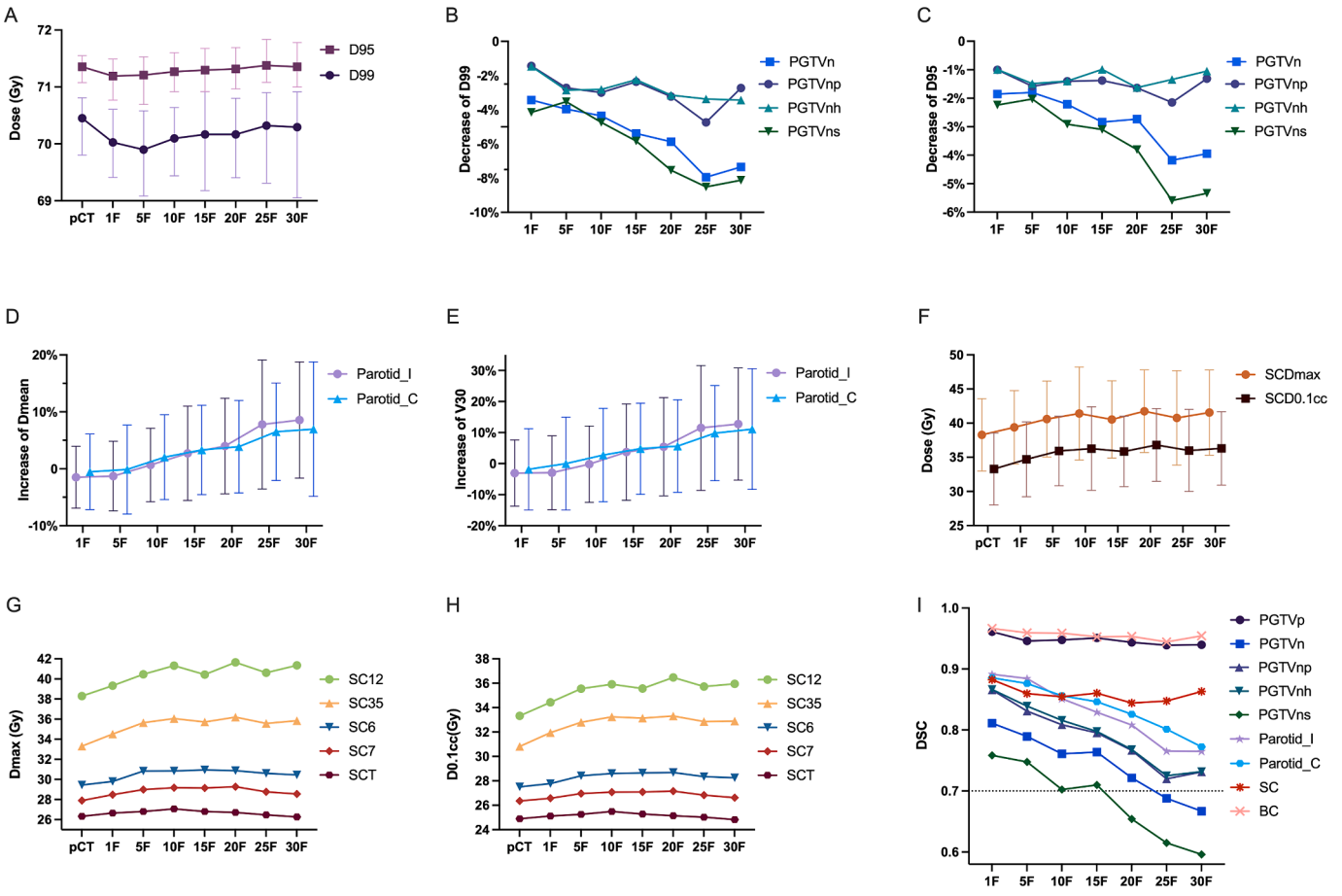

Fig. 3. Dosimetric and DSC variations. (A) Dosimetric changes in PGTVp based on median (P25, P75); (B–C) Percent decrease of D99 and D95 in PGTVn, PGTVnp (the PGTVn of positive lymph nodes), PGTVnh (the PGTVn of high-risk lymph nodes), and PGTVns (the PGTVn of suspicious lymph nodes) based on median; (D–E) Percent increase of Dmean and V30 in parotid glands based on mean ± SD; (F) Dosimetric changes in SC based on mean ± SD; (G–H) Dmax and D0.1 cc changes in SC at different segments based on mean; (F) DSC changes based on mean.

dose attenuation (P<0.001) with peaking at 25F, when D99 and D95 dropped by 7.94 % (3.28 %, 14.90 %) and 4.18 % (1.73 %, 8.40 %), respectively, from baseline (Fig. 3B–C and Table S5).

For patients with both Parotid_I and Parotid_C, the Dmean was higher for Parotid_I than for Parotid_C at baseline (30.91 ± 2.6 Gy vs. 30.11 ± 2.3 Gy; P=0.004). The delivered dose increased over time for both Parotid_I and Parotid_C (P<0.001), with the fastest increase at 25F, where the Dmean elevated by 7.80 ± 11.33 % and 6.50 ± 8.55 % from baseline, respectively (Fig. 3D–E and Table S6). However, dosimetric variations in the SC were predominantly observed before 10F (P<0.001, Fig. 3F and Table S4), with no statistically significant differences between 15F, 20F, 25F, and 30F compared to 10F (P>0.05). Notably, the increase in Dmax and D0.1 cc were more remarkable in SC12 compared to SC6 and SC7, with Dmax rising by 6.52 % vs. 2.07 % and 1.77 % at 30F from baseline (P=0.005 and P=0.001, Fig. 3G–H and Table S6). In addition, dose escalation for SCT and BC was only observed between 1F and baseline (Table S6).

DSC variations

The DSC of the PGTVp remained high at 0.95 (0.93, 0.97), even by 30F (Fig. 3I and Table S7). Nevertheless, the DSC of the PGTVn changed dramatically, dropping below to 0.69 ± 0.16 at 25F (Fig. 3I and Table S7). Although the DSC of Parotid_I and Parotid_C progressively decreased (P<0.001), the mean remained above 0.7 (Table S7 and Fig. 3I). Furthermore, a subgroup analysis showed that patients who received immunotherapy during IT had higher Parotid_I DSCs than those who did not receive immunotherapy (P=0.011, Fig. 4A). The DSC changes in SC were mainly observed in SC12 and SCT (P = 0.001 and P = 0.003), and the median DSCs were lower in SC6 and SC7 than in SC12 (0.85 and 0.87 vs.0.90 at 30F; P<0.001 and P = 0.001, respectively, Table S7).

Correlation and risk factor analysis

The correlation analysis results regarding volumetric changes, dosimetric changes, and the DSCs in the TVs and OARs during VMAT are presented in Table S8. The variation of D99 and D95 in the PGTVn exhibited a highly negative correlation with DSC (r = −0.780 and r = −0.804, P<0.001, Fig. 4B).

Previous studies have demonstrated that a 5 % reduction in the GTV dose markedly influences the local control rate (LCR) in patients with NPC [32]. In our study, the PGTVp dose remained little changed and the PGTVn dose reached its minimum during the last week of VMAT. Therefore, we established a cut-off value based on a 5 % decrease in the D95 of the PGTVn from baseline in the last week. This division resulted in two groups: Group H with a higher PGTVn dose decrease (26/60 patients) and Group L with a lower decrease (34/60 patients). The study demonstrated that patients in Group H exhibited a higher initial body mass index (BMI; 25.98 vs. 23.16 kg/m^2; P = 0.006, Fig. 4C) and a lower ORR after IT (50 % vs. 76.47 %; P=0.033, Fig. 4D) compared to Group L. The ROC curve revealed a cut-off value of 23.5 kg/m^2 for BMI (P = 0.016, Fig. 4E).

Table 2 illustrates the factors included in the logistic univariate

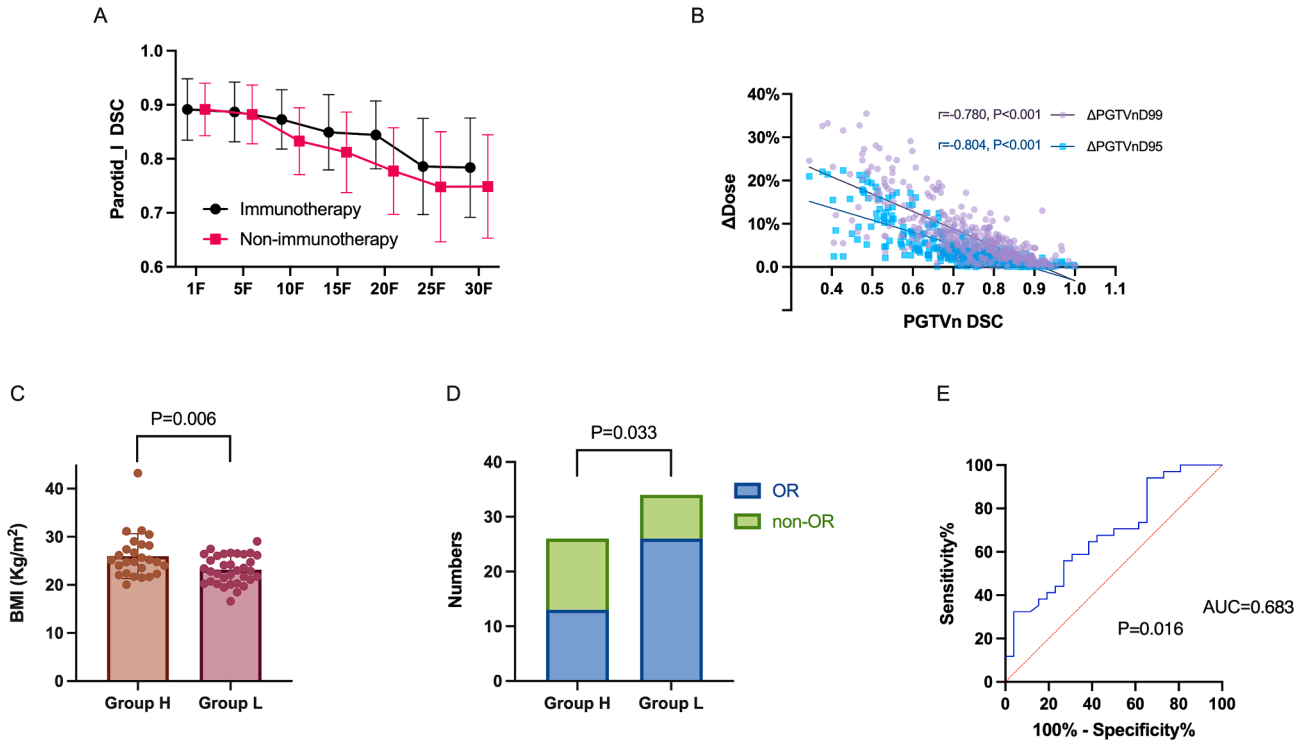

Fig. 4. Correlation analysis, subgroup analysis, and risk factor exploration. (A) Parotid_I DSC in patients treated with and without immunotherapy during IT based on mean ± SD; (B) Correlation analysis between percent dosimetric variations and DSC in PGTVn; (C) Comparison of initial BMI in Group H and Group L; (D) Comparison of objective response rates in Group H and Group L; (E) The ROC curves for predicting Group H and Group L with initial BMI.

analysis, in which those with $P<0.05$ were selected for the multivariate analysis. The multivariate analysis revealed that an initial BMI≥23.5 kg/m^2 ($P=0.034$) and not-achieving OR during IT ($P=0.045$) were independent risk factors for the Group H.

Discussion

Previous studies have explored changes in TVs and OARs during radiotherapy in LA-NPC patients receiving CCRT alone [33–35]. Currently, induction chemotherapy (IC) combined with CCRT has become the standard treatment for LA-NPC [21]. Furthermore, recent research showed that induction immuno-chemotherapy improved efficacy and survival in LA-NPC patients compared to IC, possibly due to the high expression of PD-L1 in NPC cells [36–38]. Therefore, the changing patterns of TVs and OARs during radiotherapy in post-IT LA-NPC patients remain unknown. Here, we report the anatomical and dosimetric changes during VMAT in LA-NPC patients after IT and explore characteristics of patients with notable variations for the first time.

Previous studies have highlighted a volume reduction in GTVp and GTVn ranging from 13.1–65.6 % and 28.7–72.7 %, respectively, in NPC patients during radiotherapy [8,10,33,34,39]. However, more pronounced changes in volume during IT in the present study seemed to result in smaller volume changes during VMAT. A recent study validating our perspective emphasized that IC notably mitigated weight loss and TVs reductions during CCRT, thereby decreasing anatomical and target-dose drift [23]. Meanwhile, our study revealed greater volume reductions in PGTVnp and PGTVnh, with minor reductions in PGTVns compared to PGTVn, suggesting that interference of suspicious lymph nodes may contribute to the relatively modest volumetric alternations in PGTVn.

Unlike the consensus on volumetric changes, previous studies have explored the stabilization, reduction, or increase of the GTV dose during radiotherapy [6,33–35,39–41]. Our study revealed the stabilization of PGTVp dose in post-IT patients, possibly related to smaller volume variations during VMAT as a result of IT. A notable result was the decrease in PGTVn, which was neglected in some previous studies, likely owing to small sample sizes and lack of stratification between GTVp and GTVn [6,35,39,40]. Moreover, the inconsistent dosimetric variations for PGTVp and PGTVn in our study may be explained by DSCs. Specifically, the DSC of PGTVn dropped below 0.7 at 25F, showed a strong correlation with variations in D99 and D95. This suggests that their apparent dosimetric changes were linked to greater displacement and morphology. In contrast, the DSC of the PGTVp remained above 0.9, possibly indicating dose stability during radiotherapy.

Although some studies divided the parotid glands into left and right sides or combined data from bilateral parotid glands for analysis [9,33,40], we emphasized the unequal dose received by the ipsilateral and contralateral parotid glands. Our observation of a greater baseline dose delivered to Parotid_I than to Parotid_C supports the need for separate discussions. Similar categorization models were adopted by Zhang et al. and Yao et al. [42,43]. Notably, our study maintained the mean DSC value of the parotid gland remained above 0.7 until 30F, in contrast to a previous study showed that the mean DSC value of the parotid gland dropped below 0.7 until 20F [42]. Subgroup analyses revealed a higher DSC for the Parotid_I in patients treated with immunotherapy during IT than in non-receiving patients. Immunotherapy enabled a higher ORR (72.72 %) during IT, potentially mitigating the anatomical changes caused by tumor regression during subsequent VMAT and leading to a higher parotid DSC. Moreover, compared with SC6 and SC7, SC12 showed a more pronounced increase in the delivered dose and a higher DSC, which may be related to the anatomical location and dose distribution of SC12. Specifically, the upper neck is anatomically close to the high-dose region, where slight deformation and positional changes could facilitate the SC12 migration of to the high-dose area (Fig. S1A–B). Conversely, in the lower neck, despite significant mobility [7] and smaller DSC observed in our study, the displacement had no significant effect on SC6 or SC7 dose due to their distance from the high-dose area (Fig. S1C–D).

Table 2
Possible risk factors for Group H based on logistic regression analysis.

Variables	Univariate		Multivariate	
	OR (95 %CI)	P	OR (95 %CI)	P
Age				
≥52	1.800 (0.637, 5.083)	0.267		
<52	Reference			
Gender				
Male	Reference			
Female	0.591 (0.157, 2.229)	0.437		
Initial BMI (kg/m^2)				
≥23.5	3.438 (1.145, 10.325)	0.028*	3.448 (1.099, 10.815)	0.034*
<23.5	Reference		Reference	
EBV-DNA (copies/ml)				
≥400	0.929 (0.309, 2.792)	0.896		
<400	Reference			
T stage				
T1–2	Reference			
T3–4	1.426 (0.369, 5.508)	0.607		
N stage				
N0–1	Reference			
N2–3	0.893 (0.314, 2.537)	0.832		
Clinical stage				
III	Reference			
IVA	0.595 (0.196, 1.804)	0.359		
IT regimen				
PD-1 Inhibitors	1.146 (0.398, 3.300)	0.801		
non-PD-1 Inhibitors	Reference			
initial volume of PGTVn (cc)				
≥12.4	0.271 (0.062, 1.180)	0.082		
<12.4	Reference			
volumetric reductions in PGTVn during IT (%)				
≥30.15	0.424 (0.100, 1.790)	0.243		
<30.15	Reference			
Objective response after IT				
Yes	0.308 (0.102, 0.928)	0.036*	0.312 (0.097, 0.974)	0.045*
No	Reference		Reference	

*P<0.05; EBV: epstein-barr virus; IT: induction therapy; OR: Odds Ratio; CI: Confidence Internal.

The promotion of ART is challenging in underdeveloped regions, as highly efficient devices such as TomoTherapy and Halcyon, which are capable of integrating in-room images for replanning, are only available in a few top hospitals [16,44]. Considering the progressive anatomical changes that occur in head and neck cancers during radiotherapy, offline ART has emerged as a more appropriate choice [18]. Nevertheless, the financial and human resources consumed by frequent ART may not yield commensurate clinical benefits [17,18]. Therefore, most investigations focus on exploring patterns of anatomical and dosimetry changes during radiotherapy to determine when to trigger replanning, which appears to be a more cost-effective approach to ART [16]. There is currently no consensus among NPC patients regarding the optimal timing for replanning during radiotherapy. Here, we observed that both the PGTVn and parotid doses changed most rapidly at 25F, while the spinal cord dose variation, concentrated before 10F, consistently remained within the maximum restricted dose. As a result, replanning once at 25F during VMAT has emerged as an optional ART mode for post-IT LA-NPC patients to stabilize the delivered dose.

Recent observations have argued that IC may be a risk factor for not benefiting from ART; therefore, routine replanning of all NPC patients may be overly indiscriminate [45,46]. Early identification of patients with anatomical and dosimetric instability during radiotherapy is critical for effective screening those suitable for replanning. Our study highlights the significance of PGTVn dose, as some patients experienced a dose decay of >5 %, a dosage proven to impact the LCR [32]. We propose that an initial BMI≥23.5 kg/m^2 and not-achieving OR during IT may characterize this group. Previous studies have also recognized patients with a BMI>21.5 kg/m^2 as ART candidates, yet all overlooked the impact of IT [45,47]. Notably, the introduction of not-achieving OR as a predictive factor in IT process is an innovative aspect of our study. Compared to OR patients, not-achieving OR patients experienced more noticeable anatomical variations during VMAT, reflected in greater volumetric reductions and a smaller DSC for the PGTVn (Fig. 2D–E), which may explain the attenuation of the PGTVn dose. Therefore, ART should be aggressively considered in patients with an initial BMI≥23.5 kg/m^2 and not-achieving OR during IT.

This study represents the first exploration of anatomical and dosimetric variations during VMAT in a large sample of post-IT LA-NPC patients, yielding a more comprehensive and precise pattern of variations via the stratified contours for SC and PGTVn. In contrast to previous studies that involved fewer patients undergoing IC without considering the uniqueness of it [40,43,48], our study individually analyzed post-IT patients, recognizing the impact of tumor volume reduction during IT on subsequent anatomy and dosimetry during VMAT. Meanwhile, we demonstrated significant reductions in the PGTVn dose during VMAT, initially identifying not-achieving OR during IT as a risk factor. However, this study has several limitations. Since weekly MRI scans during radiotherapy are not routine clinical practice, we were unable to obtain weekly MRI images for more accurate delineation. To mitigate this, we reconstructed CBCT images into aCT using Velocity software, ensuring positional reproducibility while providing clearer resolution for better tumor margin identification. Furthermore, owing to the retrospective nature of this study, the implementation of replanning and the acquisition of survival data were not feasible. Further investigation is needed to determine whether dosimetric attenuation translates into decreased survival and LCR.

Overall, considering the fluctuations in TVs and OARs during VMAT, 25F appears to be a feasible replanning time for post-IT LA-NPC patients. Proactive consideration of ART is recommended to maintain dose stability for individuals with an initial BMI ≥ 23.5 kg/m^2 and not-achieving OR during IT.

Ethics approval and consent to participate

Approval for this research was obtained from the Ethics Committee of Union Hospital, Tongji Medical College, Huazhong University of Science and Technology. Consent to participate was exempted due to the retrospective aspect of the study.

Funding

This work was supported by the National Key Research and Development Program of China (2016YFC0105311) and the National Natural Science Foundation of China (No. 82272901).

Declaration of competing interest

The authors declare that they have no known competing financial interests or personal relationships that could have appeared to influence the work reported in this paper.

Acknowledgments

We thank the supported from the National Key Research and Development Program of China (2016YFC0105311) and the National

Natural Science Foundation of China (No. 82272901).

Appendix A. Supplementary data

Supplementary data to this article can be found online at https://doi.org/10.1016/j.ctro.2024.100861.

References

[1] Tseng M, Ho F, Leong YH, Wong LC, Tham IW, Cheo T, et al. Emerging radiotherapy technologies and trends in nasopharyngeal cancer. Cancer Commun (lond) 2020;40(9):395–405.
[2] Chen YP, Chan ATC, Le QT, Blanchard P, Sun Y, Ma J. Nasopharyngeal carcinoma. Lancet 2019;394(10192):64–80.
[3] Wong KCW, Hui EP, Lo K-W, Lam WKJ, Johnson D, Li L, et al. Nasopharyngeal carcinoma: an evolving paradigm. Nat Rev Clin Oncol 2021;18(11):679–95.
[4] Zhang B, Mo Z, Du W, Wang Y, Liu L, Wei Y. Intensity-modulated radiation therapy versus 2D-RT or 3D-CRT for the treatment of nasopharyngeal carcinoma: a systematic review and meta-analysis. Oral Oncol 2015;51(11):1041–6.
[5] Grégoire V, Mackie TR. State of the art on dose prescription, reporting and recording in Inte nsity-Modulated Radiation Therapy (ICRU report No. 83). Cancer Radiother:. J. Soc. Franc. Radiother. Oncol. 2023;15(6-7):555-9.
[6] Chen C, Lin X, Pan J, Fei Z, Chen L, Bai P. Is it necessary to repeat CT imaging and replanning during the course of intensity-modulated radiation therapy for locoregionally advanced nasopharyngeal carcinoma? Jpn J Radiol 2013;31(9):593–9.
[7] Fung WW, Wu VW, Teo PM. Developing an adaptive radiation therapy strategy for nasopharyngeal carcinoma. J Radiat Res 2014;55(2):293–304.
[8] Yan D, Yan S, Wang Q, Liao X, Lu Z, Wang Y. Predictors for replanning in loco-regionally advanced nasopharyngeal carcinoma patients undergoing intensity-modulated radiation therapy: a prospective observational study. BMC Cancer 2013;13:548.
[9] Han C, Chen YJ, Liu A, Schultheiss TE, Wong JY. Actual dose variation of parotid glands and spinal cord for nasopharyngeal cancer patients during radiotherapy. Int J Radiat Oncol Biol Phys 2008;70(4):1256–62.
[10] Lu N, Feng LC, Cai BN, Hou J, Wang YL, Xie CB. Clinical study on the changes of the tumor target volume and organs at risk in helical tomotherapy for nasopharyngeal carcinoma. Chin Med J (engl) 2012;125(1):87–90.
[11] Yang H, Hu W, Wang W, Chen P, Ding W, Luo W. Replanning during intensity modulated radiation therapy improved quality of life in patients with nasopharyngeal carcinoma. Int J Radiat Oncol Biol Phys 2013;85(1):e47–54.
[12] Luo Y, Qin Y, Lang J. Effect of adaptive replanning in patients with locally advanced nasopharyngeal carcinoma treated by intensity-modulated radiotherapy: a propensity score matched analysis. Clin Transl Oncol 2017;19(4):470–6.
[13] Zhou X, Wang W, Zhou C, Zhu J, Ding W, Chen M, et al. Long-term outcomes of replanning during intensity-modulated radiation therapy in patients with nasopharyngeal carcinoma: an updated and expanded retrospective analysis. Radiother Oncol 2022;170:136–42.
[14] Yan D, Georg D. Adaptive radiation therapy. Z Med Phys 2018;28(3):173–4.
[15] Green OL, Henke LE, Hugo GD. Practical clinical workflows for online and offline adaptive radiation therapy. Semin Radiat Oncol 2023;29(3):219–27.
[16] Paganetti H, Botas P, Sharp GC, Winey B. Adaptive proton therapy. Phys Med Biol 2021;66:22.
[17] Wu Q, Chi Y, Chen PY, Krauss DJ, Yan D, Martinez A. Adaptive replanning strategies accounting for shrinkage in head and neck IMRT. Int J Radiat Oncol Biol Phys 2009;75(3):924–32.
[18] Glide-Hurst CK, Lee P, Yock AD, Olsen JR, Cao M, Siddiqui F, et al. Adaptive radiation therapy (ART) strategies and technical considerations: a state of the ART review from NRG oncology. Int J Radiat Oncol Biol Phys 2021;109(4):1054–75.
[19] Li WF, Chen NY, Zhang N, Hu GQ, Xie FY, Sun Y, et al. Concurrent chemoradiotherapy with/without induction chemotherapy in locoregionally advanced nasopharyngeal carcinoma: Long-term results of phase 3 randomized controlled trial. Int J Cancer 2019;145(1):295–305.
[20] Sun Y, Li WF, Chen NY, Zhang N, Hu GQ, Xie FY, et al. Induction chemotherapy plus concurrent chemoradiotherapy versus concurrent chemoradiotherapy alone in locoregionally advanced nasopharyngeal carcinoma: a phase 3, multicentre, randomised controlled trial. Lancet Oncol 2016;17(11):1509–20.
[21] Zhang Y, Chen L, Hu GQ, Zhang N, Zhu XD, Yang KY, et al. Gemcitabine and cisplatin induction chemotherapy in nasopharyngeal carcinoma. N Engl J Med 2019;381(12):1124–35.
[22] Lim AM, Corry J, Collins M, Peters L, Hicks RJ, D'Costa I, et al. A phase II study of induction carboplatin and gemcitabine followed by chemoradiotherapy for the treatment of locally advanced nasopharyngeal carcinoma. Oral Oncol 2013;49(5):468–74.
[23] Yan D, Yin X, Wang L, Huang L, Tang Q, Cheng K, et al. Induction chemotherapy reduces target volume drift in patients with locoregionally advanced nasopharyngeal carcinoma undergoing adaptive intensity-modulated radiotherapy: a retrospective cohort study. Quant Imaging Med Surg 2023;13(3):1779–91.
[24] Tang LL, Chen YP, Chen CB, Chen MY, Chen NY, Chen XZ, et al. The Chinese Society of Clinical Oncology (CSCO) clinical guidelines for the diagnosis and treatment of nasopharyngeal carcinoma. Cancer Commun (lond) 2021;41(11):1195–227.
[25] Lee AW, Ng WT, Pan JJ, Poh SS, Ahn YC, AlHussain H, et al. International guideline for the delineation of the clinical target volumes (CTV) for nasopharyngeal carcinoma. Radiother Oncol 2018;126(1):25–36.
[26] Sun Y, Yu XL, Luo W, Lee AW, Wee JT, Lee N, et al. Recommendation for a contouring method and atlas of organs at risk in nasopharyngeal carcinoma patients receiving intensity-modulated radiotherapy. Radiother Oncol 2014;110(3):390–7.
[27] van den Brekel MW, Stel HV, Castelijns JA, Nauta JJ, van der Waal I, Valk J, et al. Cervical lymph node metastasis: assessment of radiologic criteria. Radiology 1990;177(2):379–84.
[28] Hu Y, Lu T, Huang SH, Lin S, Chen Y, Fang Y, et al. High-grade radiologic extra-nodal extension predicts distant metastasis in stage II nasopharyngeal carcinoma. Head Neck 2019;41(9):3317–27.
[29] Lan M, Huang Y, Chen CY, Han F, Wu SX, Tian L, et al. Prognostic Value of cervical nodal necrosis in nasopharyngeal carcinoma: analysis of 1800 patients with positive cervical nodal metastasis at MR imaging. Radiology 2015;276(2):536–44.
[30] Balik S, Weiss E, Jan N, Roman N, Sleeman WC, Fatyga M, et al. Evaluation of 4-dimensional computed tomography to 4-dimensional cone-beam computed tomography deformable image registration for lung cancer adaptive radiation therapy. Int J Radiat Oncol Biol Phys 2013;86(2):372–9.
[31] Fotina I, Lütgendorf-Caucig C, Stock M, Pötter R, Georg D. Critical discussion of evaluation parameters for inter-observer variability in target definition for radiation therapy. Strahlenther Onkol 2012;188(2):160–7.
[32] Ng WT, Lee MCH, Chang ATY, Chan OSH, Chan LLK, Cheung FY, et al. The impact of dosimetric inadequacy on treatment outcome of nasopharyn geal carcinoma with IMRT. Oral Oncol 2014;50(5):506–12.
[33] Huang H, Lu H, Feng G, Jiang H, Chen J, Cheng J, et al. Determining appropriate timing of adaptive radiation therapy for nasopharyngeal carcinoma during intensity-modulated radiation therapy. Radiat Oncol 2015;10:192.
[34] Cheng HC, Wu VW, Ngan RK, Tang KW, Chan CC, Wong KH, et al. A prospective study on volumetric and dosimetric changes during intensity-modulated radiotherapy for nasopharyngeal carcinoma patients. Radiother Oncol 2012;104(3):317–23.
[35] Zhang X, Li M, Cao J, Luo JW, Xu GZ, Gao L, et al. Dosimetric variations of target volumes and organs at risk in nasopharyngeal carcinoma intensity-modulated radiotherapy. Br J Radiol 2012;85(1016):e506–13.
[36] Liu X, Zhang Y, Yang KY, Zhang N, Jin F, Zou GR, et al. Induction-concurrent chemoradiotherapy with or without sintilimab in patients with locoregionally advanced nasopharyngeal carcinoma in China (CONTINUUM): a multicentre, open-label, parallel-group, randomised, controlled, phase 3 trial. Lancet 2024;403(10445):2720–31.
[37] He J, Luo G, Liu S, Chen L, Chen Z, Zhang B, et al. Tislelizumab plus neoadjuvant chemotherapy and concurrent chemoradiotherapy versus neoadjuvant chemotherapy and concurrent chemoradiotherapy for locally advanced nasopharyngeal carcinoma: a retrospective study. Transl Oncol 2024;48:102058.
[38] Mai H-Q, Liu SL, Chen Q-Y, Tang L-Q, Jin F, Guo L, et al. Tislelizumab versus placebo combined with induction chemotherapy followed by concurrent chemoradiotherapy and adjuvant tislelizumab or placebo for locoregionally advanced nasopharyngeal carcinoma: Interim analysis of a multicenter, randomized, placebo-controlled, double-blind, phase 3 trial. J Clin Oncol 2024;42(16_suppl):6001.
[39] Wang RH, Zhang SX, Zhou LH, Zhang GQ, Yu H, Lin XD, et al. Volume and dosimetric variations during two-phase adaptive intensity-modulated radiotherapy for locally advanced nasopharyngeal carcinoma. Biomed Mater Eng 2014;24(1):1217–25.
[40] Jin X, Hu W, Shang H, Han C, Yi J, Zhou Y, et al. CBCT-based volumetric and dosimetric variation evaluation of volumetric modulated arc radiotherapy in the treatment of nasopharyngeal cancer patients. Radiat Oncol 2013;8:279.
[41] Yang H, Hu W, Ding W, Shan G, Wang W, Yu C, et al. Changes of the transverse diameter and volume and dosimetry before the 25th fraction during the course of intensity-modulated radiation therapy (IMRT) for patients with nasopharyngeal carcinoma. Med Dosim 2012;37(2):225–9.
[42] Zhang Y, Lin C, Wu J, Jiang X, Lee SWY, Tam SY, et al. A longitudinal evaluation of early anatomical changes of parotid gland in intensity modulated radiotherapy of nasopharyngeal carcinoma patients with parapharyngeal space involvement. J Med Radiat Sci 2017;64(3):188–94.
[43] Yao WR, Xu SP, Liu B, Cao XT, Ren G, Du L, et al. Replanning criteria and timing definition for parotid protection-based adaptive radiation therapy in nasopharyngeal carcinoma. Biomed Res Int 2015;2015:476383.
[44] Krishnatry R, Bhatia J, Murthy V, Agarwal JP. Survey on adaptive radiotherapy practice. Clin Oncol (r Coll Radiol) 2018;30(12):819.
[45] Hu YC, Tsai KW, Lee CC, Peng NJ, Chien JC, Tseng HH, et al. Which nasopharyngeal cancer patients need adaptive radiotherapy? BMC Cancer 2018;18(1):1234.
[46] Capelle L, Mackenzie M, Field C, Parliament M, Ghosh S, Scrimger R. Adaptive radiotherapy using helical tomotherapy for head and neck cancer in definitive and postoperative settings: initial results. Clin Oncol (r Coll Radiol) 2012;24(3):208–15.
[47] Brown E, Owen R, Harden F, Mengersen K, Oestreich K, Houghton W, et al. Predicting the need for adaptive radiotherapy in head and neck cancer. Radiother Oncol 2015;116(1):57–63.
[48] Tan W, Ye J, Xu R, Li X, He W, Wang X, et al. The tumor shape changes of nasopharyngeal cancer during chemoradiotherapy: the estimated margin to cover the geometrical variation. Quant Imaging Med Surg 2016;6(2):115–24.